

FIG. 2. Center-of-mass momentum spectra of π^+ and π^- mesons from the reaction $\pi^- + p \rightarrow \pi^- + \pi^+ + n$. (a) Incident pion energy $T_\pi = 1.0$ Bev. The histogram represents the data of Walker *et al.* (reference 4). (b) Incident pion energy $T_\pi = 1.37$ Bev. The histogram represents the data of Eisberg *et al.* (reference 6). In each case, the solid curve was obtained from the present isobar model. The dashed curve gives the result of the Fermi statistical theory. The two theoretical curves have been normalized to the number of observed cases.

rise in the $T = \frac{1}{2}$ cross section. A detailed consideration of the behavior at and beyond the peak would require a more detailed treatment of the process which will be presented at a later date.

One should note that more than half of the experimental^{4,6} $T = \frac{1}{2}$ cross section is inelastic. The elastic portion of the cross section contains an elastic contribution which may be composed partly of a general background and partly of the elastic diffraction scattering accompanying the inelastic cross section. The large inelastic cross section is what one expects from the pion decay of the isobar.

Feld⁷ has previously suggested the use of an isobar in these interactions to reduce the requirement for waves of high angular momentum in order to fit the magnitude of the observed peak in the $T = \frac{1}{2}$ state.

Of course one would expect this process of isobar formation to occur also in the $T = \frac{3}{2}$ state, since an isobar with $T = \frac{3}{2}$ and a pion with $T = 1$ can combine to form a $T = \frac{3}{2}$ state. It should be noted that the $T = \frac{3}{2}$ cross section $\sigma_{\frac{3}{2}}$ is increasing fairly rapidly from 0.6 Bev to ~ 1.0 Bev and reaches a peak at 1.3 Bev (see Fig. 1).

If one subtracts the tail of the low-energy resonance the effect becomes more pronounced, and suggests a lower energy threshold for the remainder of the cross section for this effect. The higher energy peak could possibly still be consistent with the formation of a $T = J = \frac{3}{2}$ isobar since the arbitrary coefficient A with which the integral of Eq. (1) is multiplied could be smaller in the $T = \frac{3}{2}$ case and hence the saturation effects for this rising integral could set in at a higher energy.

Of course the formation of a $T = \frac{5}{2}$ isobar or some other process involving production of two additional pions could occur.⁸

The predicted momentum spectra for the inelastic pion processes have been calculated⁹ for isotropic decay of the isobars, and are compared to the statistical theory and to the available experimental results^{4,6} in Figs. 2(a) and 2(b). It is clear that the predictions of the present model are in reasonable agreement with the experimental data^{4,6} within their large statistical uncertainties.

The most distinctive characteristic of these theoretical pion spectra is the double peak. The lower energy peak is due to decay pions from the isobar while the well-defined high-energy peak is due to the recoil pions. Clearly, better experimental data are needed to check these predictions accurately.

The authors are indebted to Dr. R. Serber for stimulating discussions and several important suggestions concerning this problem. We also wish to thank Dr. L. C. L. Yuan for valuable comments.

* Work performed under the auspices of the U. S. Atomic Energy Commission.

¹ Cool, Piccioni, and Clark, *Phys. Rev.* **103**, 1082 (1956); S. J. Lindenbaum and L. C. L. Yuan, *Phys. Rev.* **100**, 314 (1955).

² F. J. Dyson, *Phys. Rev.* **99**, 1037 (1955).

³ G. Takeda, *Phys. Rev.* **100**, 440 (1955).

⁴ Walker, Hushfar, and Shephard, *Phys. Rev.* **104**, 526 (1956).

⁵ S. J. Lindenbaum and R. M. Sternheimer, *Phys. Rev.* **105**, 1874 (1957).

⁶ Eisberg, Fowler, Lea, Shephard, Shutt, Thorndike, and Whittemore, *Phys. Rev.* **97**, 797 (1955).

⁷ B. T. Feld, *Proceedings of the Sixth Annual Rochester Conference on High-Energy Physics* (Interscience Publishers, Inc., New York, 1956), Chap. IV, p. 11.

⁸ K. A. Brueckner, *Proceedings of the Sixth Annual Rochester Conference on High-Energy Physics* (Interscience Publishers, Inc., New York, 1956), Chap. IV, p. 12.

⁹ After the calculations of Fig. 2 had been completed, it came to our attention that a similar calculation of the momentum spectra of pions has been carried out by Crew, Hill, and Lavatelli.

Magnetic Resonance Determination of the Magnetic Moment of the ν Meson*

T. COFFIN, R. L. GARWIN,† L. M. LEDERMAN,
S. PENMAN, AND A. M. SACHS

Columbia University, New York, New York

(Received April 17, 1957)

IN a previous experiment,¹ the g value of the positive muon was found to be $+2.00 \pm 0.10$. This is a first report on a more precise determination of the magnetic

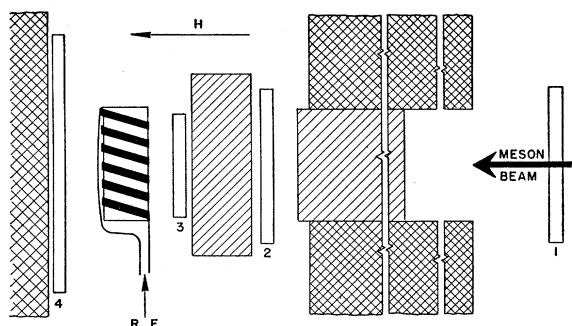


FIG. 1. Resonance apparatus for muon moment measurement. A count 1234 triggers the 12-kv rf ringing at ~ 16 Mc/sec to flip the spin of mesons stopped in the target within the coil. The variation with magnetic field of the gated counts 2314 traces out the resonance line.

moment in a magnetic resonance experiment. The g factor, with radiative corrections,² for a spin- $\frac{1}{2}$ μ meson is given by

$$g_{\mu} = 2[1 + (\alpha/2\pi) - 1.89(\alpha^2/\pi^2) + \dots]. \quad (1)$$

A measurement of g to an accuracy sufficient to establish the anomalous magnetic moment will, in addition to adding to our understanding of this particle, test the validity of quantum electrodynamics to energies $m_{\mu}/m_e \approx 200$ times higher than those involved in the anomalous contribution to the electron moment.³

The g factor (ratio of magnetic moment to spin in units of $e\hbar/2m_{\mu}c$) is given by

$$g_{\mu^+} = (m_{\mu^+}/m_p)g_p(f_{\mu^+}/f_p), \quad (2)$$

where m_{μ^+} is the muon rest mass, m_p is the proton mass, g_p is the proton g factor, and f_{μ^+}/f_p is the ratio of the resonant frequency of μ^+ mesons to that of protons in the same magnetic field.

Our present result gives

$$f_{\mu^+}/f_p = 3.1886 \pm 0.0076. \quad (3)$$

We use a proton mass of $1836.1m_e$ and for the proton g factor the value $g_p = 2(2.7927)$.⁴ The muon mass is taken to be $(206.86 \pm 0.11)m_e$.⁵ These give, for the positive muon, the result

$$g_{\mu^+} = +2.0064 \pm 0.0048 \text{ (standard deviation)}. \quad (4)$$

The technique of measurement resembles that of atomic beam experiments⁶ and the resonance measurements on positronium, since the resonance is detected not by absorption of power from an oscillator but by the change in counting rate of the decay positrons, which are strongly correlated with the direction of the muon spin.¹

The experimental arrangement is shown in Fig. 1. The magnet produces a field of 1192 gauss, uniform to $\pm 0.1\%$ over the volume of the target. The "85-Mev π^+ " beam of the Nevis Cyclotron enters the apparatus through counter 1. Most of the pions stop in the $6\frac{1}{2}$ -inch graphite absorber placed between counters

No. 1 and No. 2 in a 2-inch diameter channel bored through the pole piece of the magnet. The residual radiation has been shown to consist mostly of longitudinally polarized muons.¹

A meson which, after suffering additional energy loss in the absorber between counters No. 2 and No. 3, passes through No. 3 and stops in the target, is identified by a fast coincidence, 1234. The anticoincidence counter No. 4 (4) eliminated background due to mesons stopping in the rear poleface. Decay positrons emitted backwards are detected as 2314 coincidences, the anticoincidence requirements 1 and 4 serving primarily to eliminate beam particles and those coming from the rear poleface.

Each 1234 pulse (stopped meson) initiates two operations:

(a) It triggers the generation of a radio-frequency pulse of frequency ~ 16 Mc/sec, the amplitude of which decays exponentially with a decay constant of $1.5 \mu\text{sec}$. This pulse is applied to a coil, the axis of which is perpendicular to the dc field, producing an oscillating magnetic field of initial amplitude ~ 50 gauss in the 100-cc sample cell.

(b) The 1234 pulse also generates a gate, defining a time interval from 1.5 to $4.5 \mu\text{sec}$ after the stopping of the meson. 2314 pulses falling within this gate are recorded as electron "events." The counting rate is approximately 20 events per minute.

The measurement of the resonant transition consists of counting events per stopped meson as a function of the dc magnetic field strength. The result of a typical run is shown in Fig. 2.

The rf amplitude applied is that calculated to correspond to 100% transition probability for the μ^+ to reverse its orientation relative to the dc magnetic field, when the dc field has the value such that the μ^+ spin precession frequency is equal to the applied frequency (line center). The μ^+ is then left, after the rf pulse, with its spin opposite to the initial orientation, with the result that the original high positron counting probability ("peak" rate in the notation of reference 1)

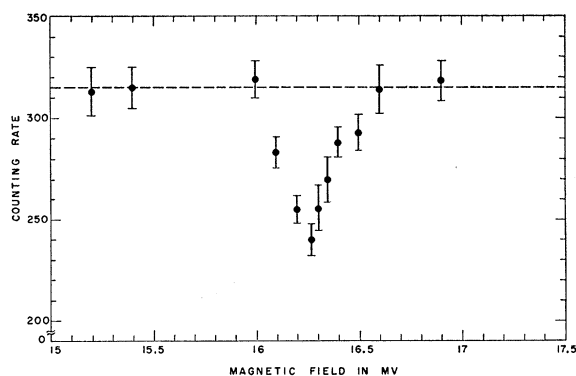


FIG. 2. Muon resonance line in the apparatus of Fig. 1. Target material: Bromoform. Proton resonance frequency at line center 5.069 ± 0.012 Mc/sec. Running time for these data: 12 hours.

is replaced by a reduced probability ("valley" rate) at the line center. The line width is limited by the breadth of the Fourier spectrum of the applied rf pulse, and the accuracy in measuring the magnetic moment, therefore, is ultimately limited for a given frequency by the finite lifetime of the muon (2.22 μ sec).

To derive the magnetic moment, the magnetic field at the line center is measured by proton magnetic resonance absorption, errors due to hysteresis and

TABLE I. Muon g values under various conditions.^a

Target material	Frequency Mc/sec	g value
CH ₂	7.5	+2.01±0.01
CHBr ₃	7.5	+2.00±0.01
Cu-(dust)	16	+2.02±0.01
Pb (in plastic)	16	+2.00±0.01
CHBr ₃	16 (3 runs)	+2.0064±0.0048

^a Errors are standard deviations which include uncertainty as to the location of line center and the distribution of stopping mesons over the volume of the sample.

influence on trajectories having been experimentally demonstrated to be negligible. The shape and central frequency of the rf spectrum are measured on a precision wave meter. The proton resonance oscillator and the wave meter are calibrated with the same crystal-checked frequency meter.

The target material had to satisfy the following conditions: long magnetic relaxation time for the μ mesons, small average internal magnetic fields, high stopping power, sufficiently low conductivity to allow the magnetic field to penetrate and to provide sufficiently small damping to allow a 1.5- μ sec ringing time. Bromoform (CHBr₃), a liquid of density 2.89 g/cm³, gave the largest line depth in this apparatus and was used most frequently. In the Bromoform run of Fig. 2, the central rf frequency was $f_\mu = 16.164 \pm 0.005$ Mc/sec, and a conventional procedure for determining the line center yields a field value at resonance corresponding to the proton resonance frequency $f_p = 5.069 \pm 0.012$ Mc/sec. The uncertainty here arises from the estimation of the line center and from the field inhomogeneity over the sample.

We have observed the resonance at several frequencies and in polyethylene, powdered copper, and leaded plastic. Table I summarizes the data. The combined best value for the 16-Mc/sec CHBr₃ runs is given in (3) above. The correction for the diamagnetism of the liquid in the target cell is negligible compared to the line width which we have thus far achieved, while the Bloch-Siegert effect in the initial rf field of 50 gauss is approximately 0.01%. It is interesting to note that a lower limit to the muon mass exists from mesonic x-ray studies⁷ which would give from (2)

$$g_{\mu+} \geq 2.0044 \pm 0.0048.$$

We are continuing these experiments with a new rf system designed to reach 140 Mc/sec at a dc field of

approximately 10 000 gauss. This will give a full line width of approximately 0.2%, thereby allowing the considerable improvement in precision which is necessary in order to observe the anomalous contribution in (1).

* Supported by the Office of Naval Research and the U. S. Atomic Energy Commission Joint Program.

† Also at International Business Machines, Watson Scientific Laboratory.

¹ Garwin, Lederman, and Weinrich, Phys. Rev. **105**, 1415 (1957). We have recently received a report from Cassels, O'Keefe, Rigby, Wetherell, and Wormald of an improved measurement of similar type with the result $g = 2.008 \pm 0.014$.

² A. Peterman, Phys. Rev. **105**, 1931 (1957); H. Suura and E. V. Wichman, Phys. Rev. **105**, 1930 (1957).

³ For recent comments on the significance of the muon moment in quantum electrodynamics, see Berestetskii, Krokhn, and Khlebnikov, J. Exptl. Theoret. Phys. (S.S.S.R.) **30**, 788 (1956) [translation: Soviet Phys. JETP **3**, 761 (1956)].

⁴ Hipple, Sommer, and Thomas, Phys. Rev. **82**, 697 (1951).

⁵ Cohen, Crowe, and DuMond (to be published).

⁶ I. I. Rabi, Phys. Rev. **51**, 652 (1936).

⁷ Koslov, Fitch, and Rainwater, Phys. Rev. **95**, 625 (1954).

Polarization of Electrons in Muon Decay and the Two-Component Theory of the Neutrino*

TOICHIRO KINOSHITA AND ALBERTO SIRLIN

Laboratory of Nuclear Studies, Cornell University, Ithaca, New York

(Received April 16, 1957)

RECENTLY, Lee and Yang, Salam, and Landau have proposed independently a two-component theory of the neutrino.¹ The significance of this theory for muon decay has been studied on the basis of the general four-component theory.² The effect of the radiative correction has also been discussed.² In this note, we want to point out that the longitudinal polarization of an electron emitted from a muon at rest gives further information about the nature of the muon decay interaction in the two-component theory.

The muon decay is described in the two-component theory by a Hamiltonian

$$g_V(\bar{\psi}_\mu \gamma_\rho \psi_e)(\bar{\psi}_\nu \gamma_\rho \psi_\nu) + g_A(\bar{\psi}_\mu(-i\gamma_\rho \gamma_5)\psi_e) \times (\bar{\psi}_\nu(-i\gamma_\rho \gamma_5)\psi_\nu) + \text{H.c.}, \quad (1)$$

where ψ_ν satisfies

$$\gamma_5 \psi_\nu = -\psi_\nu, \quad (2)$$

and H.c. is the Hermitian conjugate. Because of (2), the interaction can be expressed in the form

$$(\bar{\psi}_\mu \gamma_\rho [g_V + g_A \gamma_5] \psi_e)(\bar{\psi}_\nu \gamma_\rho \psi_\nu) + \text{H.c.}, \quad (3)$$

where $g_V + g_A \gamma_5$ may be written as

$$(g_V - g_A) \frac{1 - \gamma_5}{2} + (g_V + g_A) \frac{1 + \gamma_5}{2}. \quad (4)$$

Let us note that, in the case where the electron mass is negligible compared with its momentum, the operator